$[(Cp-CMe_2-Flu)_2Ln]^-[Li(ether)_n]^+$ (Ln = Y, La): Complexes with Unusual Coordination Modes of the Fluorenyl Ligand and the First Examples of Bis-Ansa Lanthanidocenes

Evgueni Kirillov,[†] Loic Toupet,[‡] Christian W. Lehmann,[§] Abbas Razavi,[∥] Samia Kahlal,[⊥] Jean-Yves Saillard,*[,⊥] and Jean-François Carpentier*[,†,#]

Organométalliques et Catalyse, UMR 6509 CNRS-Université de Rennes 1, Institut de Chimie de Rennes, 35042 Rennes Cedex, France, Groupe Matière Condensée et Matériaux, Cristallochimie, UMR 6626 CNRS-Université de Rennes 1, 35042 Rennes Cedex, France, Max-Planck-Institut für Kohlenforschung, Chemical Crystallography, Postfach 101353, 45466 Mülheim/Ruhr, Germany, Atofina Research, Zone Industrielle C, 7181 Feluy, Belgium, and Chimie du Solide et Inorganique Moléculaire, UMR 6511 CNRS-Université de Rennes 1, Institut de Chimie de Rennes, 35042 Rennes Cedex, France

Received March 10, 2003

Salt metathesis reactions between $LnCl_3(THF)_n$ (Ln = Y, La) and 1 equiv of the dilithium salt of the isopropylidene-bridged ligand $[Flu-CMe_2-Cp]Li_2$ (Flu = fluorenyl), in diethyl ether solution, led to the isolation of new ionic metallocene complexes, $[(Cp-CMe_2-Flu)_2Ln]^-[Li(ether)_n]^+$ (ether = Et_2O, THF; Ln = Y, n = 4, **2**; Ln = La, n = 2, **3**), which contain two chelating ligand units per metal center. The ionic complex **2** presumably originates from ligand redistribution in the primary formed heteroleptic ate complex $[(Cp-CMe_2-Flu)YCl_2]^-[Li(ether)_4]^+$ (**1**) upon crystallization. Complex **2** was selectively prepared on using 2 equiv of $[Cp-CMe_2-Flu]Li_2$ vs $YCl_3(THF)_{3.5}$. The solid-state structures of **2** and **3** were established by X-ray diffraction studies. Three polymorphic varieties of **2** were identified and all shown to correspond to a fully dissociated ion pair with the formula $[(\eta^3{:}\eta^5\text{-}Flu-CMe_2-Cp)(\eta^1{:}\eta^5\text{-}Flu-CMe_2-Cp)Y]^-[Li(Et_2O)(THF)_3]^+$ (**2**). The fluorenyl ligands in **2** show an unprecedented η^1 bonding mode and a rare η^3 bonding mode involving, respectively, a carbon atom of a phenyl ring and the bridgehead carbon atom of the central ring and the two adjacent carbon atoms of one six-membered ring. DFT computations carried out on the anionic fragment of **2** corroborated the nature of these bonding modes. Only the last exocyclic η^3-bonding mode is observed for the fluorenyl moieties in complex **3**, which features an associated ion-pair structure with the formula $[(\eta^3{:}\eta^5\text{-}Flu-CMe_2-Cp)_2La]^-[Li(OEt_2)_2]^+$. For comparison purposes, the isopropylidene-bridged bis(indenyl) complex $[(Ind-CMe_2-Ind)_2Y]^-[Li(THF)_4]^+$ (**4**) was synthesized by a salt metathesis procedure and characterized by X-ray diffraction. In contrast to fluorenyl-containing complexes **2** and **3**, only the cyclopentadienyl rings of the indenyl moieties coordinate to yttrium in **4**. Ionic complexes **2**−**4** constitute the first structurally characterized examples of bis-ansa lanthanidocenes.

Introduction

Over the past 20 years, a large variety of group 3 and group 4 *ansa*-metallocenes combining cyclopentadienyl, indenyl, and fluorenyl rings linked by one-atom or two-atom carbon or silicon bridges has been prepared.[1] Those complexes have attracted considerable interest, in particular due to their catalytic abilities in α-olefin polymerization.[2] Recently, efforts have been made to prepare *ansa*-lanthanidocenes based on single-carbon-bridged cyclopentadienyl/fluorenyl systems, $[Cp-CR_2-Flu]$, which have played a unique role in group 4 metal chemistry.[3] Qian et al. have shown that salt metathesis reactions of $[Cp-CPh_2-Flu]M_2$ (M = Li, K) with $LnCl_3(THF)_n$ (Ln = Y, Lu) and $Ln(BH_4)_3(THF)_3$ (Ln = La, Nd) give the ionic complexes $[(\eta^5{:}\ \eta^5\text{-}Cp-CPh_2-Flu)LnCl_2]^-[Li(THF)_4]^+$ and $[(Cp-CPh_2-Flu)Ln((\mu\text{-}H)_3BH)_2]^-[Li(THF)_4]^+$, respectively.[4] It has been shown that amine

[†] Organométalliques et Catalyse, Université de Rennes 1.
[‡] Groupe Matière Condensée et Matériaux, Université de Rennes 1.
[§] Max-Planck-Institut für Kohlenforschung.
[∥] Atofina Research.
[⊥] Chimie du Solide et Inorganique Moléculaire, Université de Rennes 1.
[#] Fax: (+33)(0)223-236-939. E-mail: jean-francois.carpentier@univ-rennes1.fr.

(1) For pioneering articles see: (a) Smith, J. A.; Seyerl, J. V.; Huttner, G.; Brintzinger, H. H. *J. Organomet. Chem.* **1979**, *173*, 175. (b) Kaminsky, W.; Külper, K.; Brintzinger, H. H. Wild, F. R. W. P. *Angew. Chem., Int. Ed. Engl.* **1985**, *24*, 507. For a recent review see: (c) Shapiro, P. *Coord. Chem. Rev.* **2002**, *231*, 67 and references therein.

(2) For reviews see: (a) Jordan, R. F. *Adv. Organomet. Chem.* **1991**, *32*, 325. (b) Brintzinger, H. H.; Fischer, D.; Mulhaupt, R.; Rieger, B.; Waymouth, R. M. *Angew. Chem., Int. Ed. Engl.* **1995**, *34*, 1143. (c) Bochmann, M. *J. Chem. Soc., Dalton Trans.* **1996**, 255. (d) Kaminsky, W. *J. Chem. Soc., Dalton Trans.* **1998**, 1413. (e) Alt, H. G.; Köppl, A. *Chem. Rev.* **2000**, *100*, 1205. (f) Coates, G. W. *Chem. Rev.* **2000**, *100*, 1223. (g) Hou, Z.; Wakatsuki, Y. *Coord. Chem. Rev.* **2002**, *231*, 1.

(3) (a) Ewen, J. A.; Jones, R. L.; Razavi, A.; Ferrara, J. D. *J. Am. Chem. Soc.* **1988**, *110*, 6255. (b) Razavi, A.; Ferrara, J. *J. Organomet. Chem.* **1992**, *435*, 299. (c) Drago, D.; Pregosin, P. S.; Razavi, A. *Organometallics* **2000**, *19*, 1802 and references therein.

10.1021/om030181o CCC: $25.00
Publication on Web 08/23/2003

elimination reactions of homoleptic amides Ln[N(SiMe$_3$)$_2$]$_3$ (Ln = Y, La, Nd) with the isopropylidene-bridged CpH−CMe$_2$−FluH ligand lead to the formation of *ansa*-metallocenes (η^5:η^5-Cp−CMe$_2$−Flu)Ln(η^5-Cp−CMe$_2$−FluH), instead of the desired products (η^5:η^5-Cp−CMe$_2$−Flu)Ln[N(SiMe$_3$)$_2$].[5] Here we report the synthesis and structural characterization of a new type of ionic metallocene complex that contains *two* chelating ligand units [Cp−CMe$_2$−Flu]$^{2-}$ per metal center. Both the cyclopentadienyl and the fluorenyl moieties effectively coordinate to the metal center, but the fluorenyl ligands show unusual, nonsymmetric bonding modes.

Results and Discussion

Salt Metathesis Reactions of [Cp−CMe$_2$−Flu]Li$_2$ and LnCl$_3$(THF)$_n$ (Ln = Y, La). Our initial attempts in this chemistry were conducted with the aim of preparing neutral or ionic chloro−lanthanidocene complexes of the type "[Cp−CMe$_2$−Flu]LnCl" or "{[Cp−CMe$_2$−Flu]LnCl$_2$}$^-$", for further transmetalation with lithiated reagents to attain potentially valuable amido and carbyl derivatives.[4c] Accordingly, salt metathesis reactions were first performed using *1* equiv of [Cp−CMe$_2$−Flu]Li$_2$ vs LnCl$_3$(THF)$_n$ precursors (Ln = Y, La).

The highly air-sensitive dark red product **1** obtained from YCl$_3$(THF)$_{3.5}$ under those conditions using diethyl ether as solvent is not soluble in pentane, sparingly soluble in toluene, moderately soluble in Et$_2$O, and readily soluble in THF, suggesting an ionic structure. Elemental analysis of crude **1** and its reactivity in solution[6] were consistent with the general formula [(Cp−CMe$_2$−Flu)YCl$_2$]$^-$[Li(ether)$_4$]$^+$ (ether = THF, Et$_2$O): i.e., a bulk composition similar to that of ionic lanthanide complexes obtained from salt metathesis reactions using the diphenylmethylene-bridged analogue ligand [Cp−CPh$_2$−Flu].[4] However, X-ray microfluorescence analysis of solid **1** showed that it contained in fact two phases, with Cl to Y ratios of 0 ± 0.2 and 4 ± 0.2, respectively. Also, X-ray diffraction studies of several suitable single crystals with different shapes isolated from several recrystallization batches demonstrated they all have the same ionic, chlorine-free formula [(Flu−CMe$_2$−Cp)$_2$Y]$^-$[Li(Et$_2$O)(THF)$_3$]$^+$ (**2**) (vide infra). No crystal corresponding to the structure expected for **1** could be isolated, despite repeated efforts. These results suggest that the heteroleptic ate complex [(Cp−CMe$_2$−Flu)YCl$_2$]$^-$[Li(ether)$_4$]$^+$ (**1**), which is expected to be the primary product formed in the 1:1 salt metathesis,[4] undergoes upon crystallization a disproportionation reaction to yield a 1:1 mixture of homoleptic complex **2** and [YCl$_4$]$^-$ (Scheme 1). Such ligand redistribution processes are indeed quite common in lanthanide chemistry.[7,8]

Likewise, salt metathesis experiments conducted from LaCl$_3$(THF)$_{1.5}$ and *1* equiv of [Cp−CMe$_2$−Flu]Li$_2$ led to

Scheme 1. Proposed Disproportionation Mechanism for the Formation of 2 from the 1:1 Salt Metathesis Reaction of YCl$_3$(THF)$_{3.5}$ and [Cp−CMe$_2$−Flu]Li$_2$ (ether = THF, Et$_2$O).

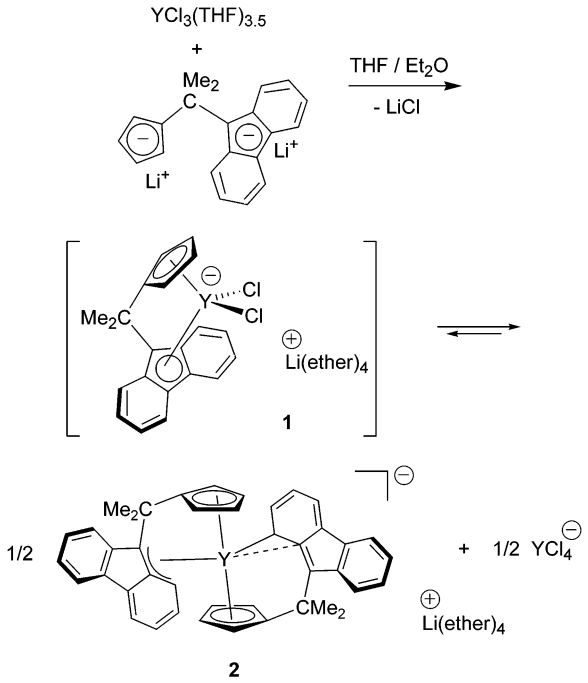

the isolation of pink crystals of the ionic complex [(Flu−CMe$_2$−Cp)$_2$La]$^-$[Li(Et$_2$O)$_2$]$^+$ (**3**) in 42% yield (vs ligand) (eq 1). This complex is more sensitive, both in solution

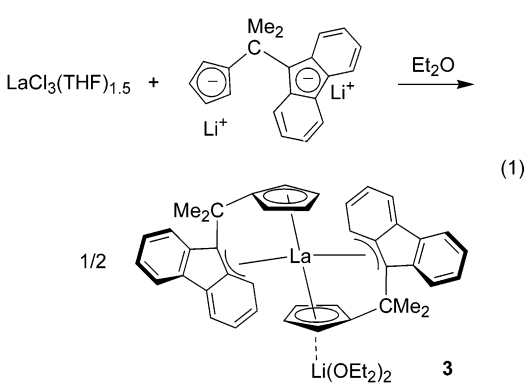

and in the solid state, than its yttrium analogue **2** but could be stored without significant decomposition at least for weeks under argon at −30 °C. These results show that, despite the large difference in the ionic radii of yttrium and lanthanum,[9] both metals induce the formation of similar ionic complexes that contain *two* mixed chelating units [Cp−CMe$_2$−Flu] per metal center. This evidences, for this series of isopropylidene-bridged

(4) (a) Qian, C.; Nie, W.; Sun, J. *J. Chem. Soc., Dalton Trans.* **1999**, 3283. (b) Qian, C.; Nie, W.; Sun, J. *J. Organomet. Chem.* **2001**, *626*, 171. (c) Qian, C.; Nie, W.; Chen, Y.; Jie, S. *J. Organomet. Chem.* **2002**, *645*, 82. (d) Nie, W.; Qian, C.; Chen, Y.; Jie, S. *J. Organomet. Chem.* **2002**, *647*, 114.

(5) Dash, A. K.; Razavi, A.; Mortreux, A.; Lehmann, C. W.; Carpentier, J.-F. *Organometallics* **2002**, *21*, 3238.

(6) Reaction of **1** with alkyllithium reagents LiR (R = CH$_2$SiMe$_3$, CH(SiMe$_3$)$_2$, etc.) proceeds cleanly to give the corresponding neutral hydrocarbyl complexes (η:η-Flu−CMe$_2$−Cp)Y(R)(THF)$_n$ in high yields with elimination of LiCl: Kirillov, E.; Razavi, A.; Toupet, L.; Lehmann, C. W.; Carpentier, J.-F. Manuscript in preparation.

(7) Recent organolanthanide reviews: (a) Schumann, H.; Meese-Marktscheffel, J. A.; Esser, L. *Chem. Rev.* **1995**, *95*, 865. (b) Anwander, R.; Herrmann, W. A. *Top. Curr. Chem.* **1996**, *179*, 1. (c) Edelmann, F. T. *Top. Curr. Chem.* **1996**, *179*, 247. (d) Anwander, R. In *Applied Homogeneous Catalysis with Organometallic Compounds*; Cornils, B., Herrmann, W. A., Eds.; Wiley: Weinheim, Germany, 1996; Vol. 2, p 866. (e) Anwander, R. *Top. Organomet. Chem.* **1999**, *2*, 1. (f) Molander, G. A.; Dowdy, E. C. *Top. Organomet. Chem.* **1999**, *2*, 119. (g) Arndt, S.; Okuda, J. *Chem. Rev.* **2002**, *102*, 1953. (h) Hou, Z.; Wakatsuki, Y. *Coord. Chem. Rev.* **2002**, *231*, 1

(8) See for example: Roesky, P. W. *Organometallics* **2002**, *21*, 4756.

(9) Effective ionic radii for eight-coordinate metal centers: La^{3+}, 1.160 Å; Y^{3+}, 1.019 Å; Zr^{4+}, 0.84 Å. Shannon, R. D. *Acta Crystallogr., Sect. A* **1976**, *A32*, 751.

Table 1. Crystal Data and Structure Refinement Details

	monoclinic **2**	triclinic **2**·0.5Et_2O	orthorhombic **2**	**3**	**4**·THF
formula	$C_{58}H_{70}LiO_4Y$	$C_{60}H_{75}LiO_{4.5}Y$	$C_{58}H_{70}LiO_4Y$	$C_{50}H_{56}LaLiO_2$	$C_{62}H_{76}LiO_5Y$
cryst size, mm	0.18 × 0.05 × 0.03	0.24 × 0.20 × 0.10	0.22 × 0.22 × 0.08	0.08 × 0.08 × 0.07	0.38 × 0.33 × 0.33
M_r	927.02	964.05	927.02	834.84	997.08
cryst syst	monoclinic	triclinic	orthorombic	triclinic	monoclinic
space group	*Cc*	$P\bar{1}$	$Pca2_1$	*P*1	*Cc*
a, Å	10.5879(3)	12.599(2)	19.1523(7)	11.4499(4)	10.7603(2)
b, Å	32.1072(8)	13.398(3)	10.1817(4)	12.7450(4)	26.9403(5)
c, Å	14.2001(3)	17.133(4)	24.7512(12)	15.1546(6)	17.8960(3)
α, deg	90	67.74(2)	90	90.8680(10)	90
β, deg	92.7450(10)	70.540(10)	90	98.0390(10)	92.6040(10)
γ, deg	90	74.977(8)	90	115.615(3)	90
V, Å^3	4821.8(2)	2494.2(9)	4826.6(3)	1967.46(12)	5184.0(2)
Z	2	2	4	2	4
D_{calcd}, Mg m^{-3}	1.277	1.284	1.277	1.443	1.278
T, K	120(2)	120(2)	120(2)	100(2)	120(2)
θ range, deg	2.43−27.50	2.58−21.93	3.82−24.95	1.78−27.55	2.29−27.54
μ, mm^{-1}	1.256	1.218	1.255	1.128	1.175
no. of measd rflns	30 810	9487	26 524	15 950	5950
no. of indep rflns	10 914	5174	8274	8636	5950
no. of rflns with $I > 2\sigma(I)$	8792	4220	4686	6701	5590
no. of params	520	580	590	495	623
goodness of fit	1.025	1.123	1.016	1.120	1.057
R1 ($I > 2\sigma(I)$)	0.0858	0.0775	0.0921	0.0894	0.0582
wR2	0.2185	0.1924	0.1943	0.1896	0.1578
largest diff, e Å^{-3}	1.09	1.03	0.58	0.980/−2.105	1.066/−0.682

complexes, the general relative higher stability, at least in the solid state, of homoleptic species $[(Flu-CMe_2-Cp)_2Ln]^-[Li(ether)_n]^+$ versus the corresponding heteroleptic species "$[Cp-CMe_2-Flu]LnCl$" or "$\{[Cp-CMe_2-Flu]LnCl_2\}^-$", in striking opposition to parent complexes based on the $[Cp-CPh_2-Flu]$ ligand system.[4]

Not surprisingly, considering its stoechiometry, yttrium compound **2** was further selectively prepared as dark red crystals in 70% isolated yield on using *2* equiv of $[Cp-CMe_2-Flu]Li_2$ vs $YCl_3(THF)_{3.5}$ (eq 2). Consistent

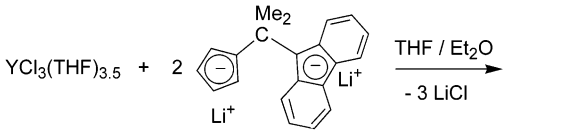

(2)

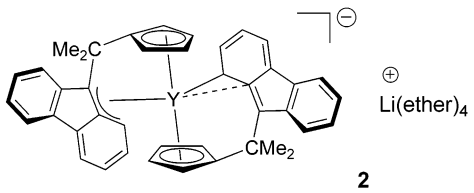

2

with its ionic structure, complex **2** is poorly soluble in aromatic and aliphatic hydrocarbons and highly soluble in ether solvents. This product is highly sensitive to moisture and prone to rapid hydrolysis. Thus, ^{1}H NMR monitoring of a solution of **2** in not fully dried THF at room temperature showed the rapid formation of the neutral complex $(\eta^5{:}\eta^5\text{-}Cp-CMe_2-Flu)Ln(\eta^5\text{-}Cp-CMe_2-FluH)$.[5]

Isopropylidene-Bridged *ansa*-Bis(2-indenyl) System. To enlarge the scope of these new anionic sterically constrained lanthanidocene complexes and to investigate in particular the influence of the nature of the ansa ligand on the coordination mode, the yttrium complex derived from an isopropylidene-bridged *ansa*-bis(2-indenyl) ligand was prepared. The anionic complex **4**, $[(Ind-CMe_2-Ind)_2Y]^-[Li(ether)_4]^+$, was synthesized by reacting 2 equiv of the dilithium salt $[(2\text{-}Ind)-CMe_2-(2\text{-}Ind)]Li_2$ with $YCl_3(THF)_{3.5}$ in diethyl ether and isolated as a yellow crystalline solid in 82% yield (eq 3). Complex **4** is quite more stable than fluorenyl

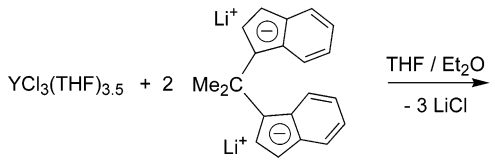

(3)

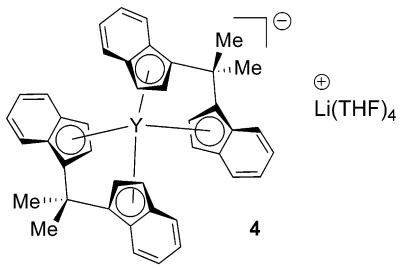

4

derivatives **2** and **3**, both in solution and in the solid state, and was fully characterized by NMR, elemental analysis, and an X-ray diffraction study of single crystals grown from a THF/Et_2O solution. This anionic compound is soluble in THF and very poorly soluble in hydrocarbons (pentane, toluene). Its ^{1}H NMR spectra in THF-d_8, both at room temperature and −70 °C, showed only one set of sharp resonances (six signals for the indenyl groups and one signal for the CMe_2 bridge) corresponding to a symmetrically coordinated species on the NMR time scale.

Solid-State Structures of the Ionic Complexes $[(Flu-CMe_2\text{-}Cp)_2Y]^-[Li(Et_2O)(THF)_3]^+$ (2), $[(Flu-CMe_2-Cp)_2La]^-[Li(Et_2O)_2]^+$ (3), and $[(Ind-CMe_2-Ind)_2Y]^-[Li(THF)_4]^+(THF)$ (4). The solid-state structures of the new anionic complexes **2**−**4** were established by X-ray diffraction studies (Table 1). Most interestingly, all the recrystallized samples of **2** we prepared were found to contain three polymorphic varieties of **2**; i.e., the crystal shape, space group, and cell parameters are different but the general atom connectivity and bonding features of the three crystal structures are essentially the same. Nevertheless, noticeable differ-

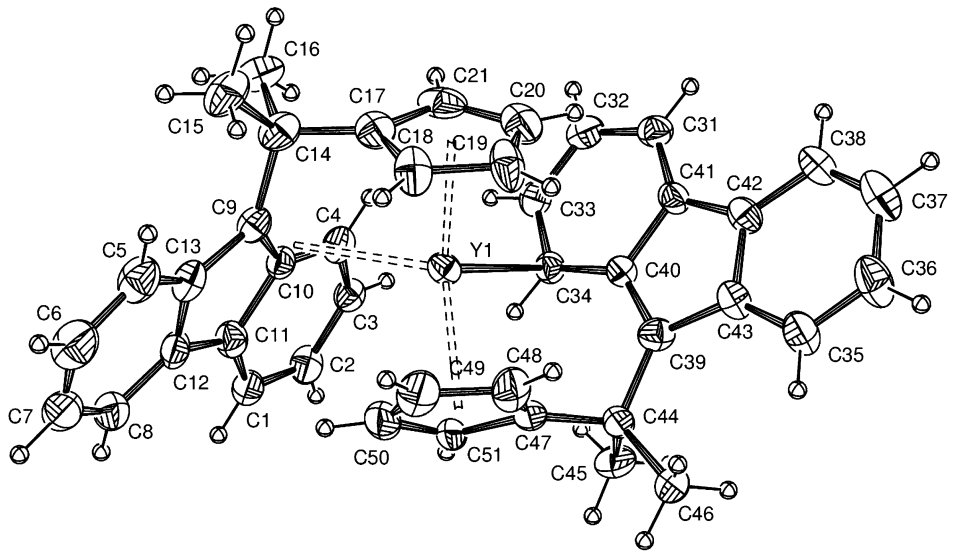

Figure 1. ORTEP drawing of the anion of $[(\eta^3{:}\eta^5\text{-Flu}-CMe_2-Cp)(\eta^1{:}\eta^5\text{-Flu}-CMe_2-Cp)Y]^-[Li(Et_2O)(THF)_3]^+$ (**2**, monoclinic form) Ellipsoids correspond to 50% probability.

Table 2. Selected Bond Distances (Å) and Angles (deg) for Polymorphs of 2 and Complex 3

	monoclinic **2**	triclinic **2**	orthorhombic **2**	**3**
Ln(1)−C(4)	2.690(7)	2.782(8)	2.789(12)	3.026(7)
Ln(1)−C(10)	2.806(7)	2.749(8)	2.796(12)	2.881(7)
Ln(1)−C(9)	3.065(8)	2.894(8)	2.945(13)	3.054(7)
Ln(1)−C(34)	2.722(6)	2.671(8)	2.694(13)	2.965(6)
Ln(1)−C(40)	3.101(7)	3.177(8)	3.143(13)	2.891(7)
Ln(1)−C(39)	3.540(8)	3.723(8)	3.633(12)	3.077(6)
Ln(1)−C(17−21)[a]	2.601(8)	2.611(8)	2.624(12)	2.835(7)
Ln(1)−C(47−51)[a]	2.645(8)	2.606(8)	2.629(11)	2.772(7)
Cp(1)−Ln(1)−Cp(2)[b]	130.00	128.77	130.98	125.05
Cp(1)−Ln(1)−allyl[b,c]	95.12	95.06	94.84	86.91
Cp(2)−Ln(1)−C(34)[b]	101.76	99.65	98.72	89.29
C(9)−C(14)−C(17)	108.4(6)	107.5(7)	108.9(9)	108.2(5)
C(39)−C(44)−C(47)	109.1(6)	108.5(7)	109.7(10)	108.3(5)

[a] Average Ln−C(Cp) bond distances. [b] Cp(1) = Cp centroid of C(17−21); Cp(2) = Cp centroid of C(47−51). [c] allyl = allyl centroid of [C(4)−C(9)−C(10)].

ences in the geometric parameters (bond lengths and angles, Table 2) do exist between these polymorphs, which arise from the large flexibility of this molecule (vide infra). Complex **2** comprises a fully dissociated ion pair in the solid state. The cation is composed by a lithium atom coordinated by four ether molecules, as observed in other ionic lanthanidocenes.[4] In contrast, the anion has an unprecedented structure with the yttrium atom coordinated in a distorted-tetrahedral geometry by two nonequivalent [Flu−CMe_2−Cp] ligand units (Figure 1). To the best of our knowledge, this represents the first structurally characterized example of an early-transition-metal sandwich complex with two ansa Cp-type ligands.[10] Furthermore, the bonding of the fluorenyl moieties in **2** is unexpected. Chart 1 shows various potential bonding modes of fluorenyl ligands found in ansa and simple metallocenes of zirconium and lanthanides previously established by X-ray diffraction studies.[11] In most complexes the metal is essentially symmetrically bonded to the five-membered ring of the fluorenyl ligand: η^5 bonded (**A**), e.g. in ($\eta^5{:}\eta^5$-Cp−CMe_2−Flu)$ZrCl_2$[3b] and ($\eta^5{:}\eta^5$-Cp−$SiMe_2$−Flu)$Y(N(SiMe_3)_2)$,[12] η^3 bonded (**B**), e.g. in ($\eta^5{:}\eta^3$-Flu)$_2$Sm(THF)$_2$[13] and ($\eta^5{:}\eta^3$-

Chart 1. Bonding Modes of Fluorenyl Moieties Observed in *ansa*-Metallocenes (A−E; M = Zr, Y, Sm), in $[(Flu-CMe_2-Cp)_2Y]^-[Li(OEt_2)(THF)_3]^+$ (2; D + E), and in $[(Flu-CMe_2-Cp)_2La]^-[Li(OEt_2)_2]^+$ (3; E)

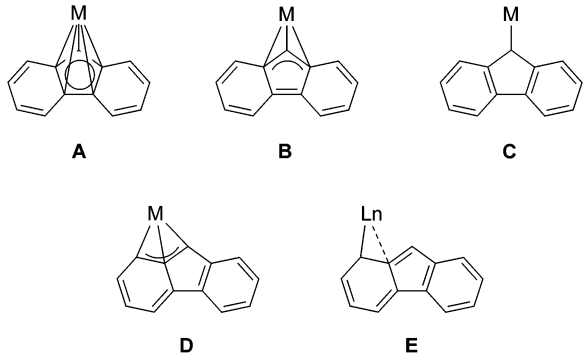

Cp−$SiMe_2$−Flu)$YCl_2Li(OEt_2)_2$,[12] or, more seldomly, η^1 bonded (**C**), as in (η^5-$C_5H_4Me)_2Zr(\eta^1$-$C_{13}H_9)(Cl)$.[14] An unusual exocyclic η^3-allyl bonding mode (**D**) involving the bridgehead carbon atom of the central ring and the two adjacent carbon atoms of one six-membered ring has

(10) (a) Ionic $[(\pi\text{-}C_5H_5)_3Ln(\mu,\sigma\text{-}C_5H_5)Na(THF)_n]$ complexes (Ln = La, Ce, Pr, Nd; n = 0, 1) have been prepared and characterized by elemental analysis and NMR: Jacob, K.; Glanz, M.; Tittes, K.; Thiele, K. H.; Pavlik, I.; Lycka, A. *Z. Anorg. Allg. Chem.* **1989**, *577*, 145. (b) Synthesis and X-ray characterization of $[(\eta^5\text{-}C_5H_5)_3NdPh][Li(DME)_3]$: Gao, H.; Shen, Q.; Hu, J.; Jin, S.; Lin, Y. *J. Organomet. Chem.* **1992**, *427*, 141. (c) Synthesis and X-ray characterization of $Li[(\eta^5\text{-}C_5H_5)_2Y\text{-}(\mu,\eta^1\text{-FcN})_2]$ (FcN = 2-dimethylaminoferrocenyl): Jacob, K.; Schäfer, M.; Steiner, A.; Sheldrick, G. M.; Edelmann, F. T. *J. Organomet. Chem.* **1995**, *487*, C18. Examples of ionic, nonmetallocene lanthanide complexes that contain two chelating ligand units have also been reported: (d) $Li[Ln(\eta^5{:}\eta^1\text{-}C_5H_3t\text{BuSiMe}_2NCH_2CH_2X)_2]$ (Ln = Y, Lu): Hultzsch, K. C.; Spaniol, T. P.; Okuda, J. *Organometallics* **1997**, *16*, 4845. (e) $[Lu\{ArN(CH_2)_3NAr\}_2]^-[LuCl_2(THF)_5]^+$: see ref 8.

(11) Arene type η^6 coordination of fluorenyl ligands by the six-membered rings has been also observed in the solid state. (a) Bimetallic lanthanide−aluminum complexes $[(\eta^6\text{-}Me_3Si-\text{fluorene})AlMe_3]_2Sm$ and $[(\eta^6\text{-}Me_3Si-\text{fluorene})AlMe_3]Sm[\eta^5\text{-}Me_3Si-\text{fluorenyl}]$: Nakamura, H.; Nakayama, Y.; Yasuda, H.; Maruo, T.; Kanehisha, N.; Kai, Y. *Organometallics* **2000**, *19*, 5392. (b) Fluorenyllithium $(\eta^6\text{-FluLi})_2$: Üffing, C.; Köppe, R.; Schnöckel, H. *Organometallics* **1998**, *17*, 3512.

(12) Lee, M. H.; Hwang, J.-W.; Kim, Y.; Kim, J.; Han, Y.; Do, Y. *Organometallics* **1999**, *18*, 5124.

(13) Evans, W. J.; Gummersheimer, T. S.; Boyle, T. J.; Ziller, J. W. *Organometallics* **1994**, *13*, 1281.

(14) Schmid, M. A.; Alt, H. G.; Milius, W. *J. Organomet. Chem.* **1997**, *541*, 3.

been presented by Bochmann et al. in [(η^5:η^3-Cp−CMe_2−Flu)Zr(μ-H)(Cl)]$_2$, with Zr−C bond distances in the range 2.608(3)−2.686(3) Å.[15,16] This last exocyclic η^3-bonding mode is found for one of the two fluorenyl moieties of the three polymorphs of **2**. In the triclinic polymorph, the η^3 coordination of the fluorenyl ligand is found to be quite symmetric and approaches Bochmann's case (**D**), as shown by the minimal distance of 2.749(8) Å with the central allyl C(10) atom and the 0.112 Å difference between the bond distances of Y with the two terminus carbon atoms (Δ(Y−C(9)/Y−C(4)). In contrast, the monoclinic and orthorhombic polymorphs of **2** feature a dissymmetric coordination for this η^3-bonded fluorenyl, the yttrium atom being tilted on one side of the fluorenyl system, with Y−C(4) in the range 2.690(7)−2.789(12) Å, Y−C(10) in the range 2.796(12)−2.806(8) Å, and Y−C(9) in the range 2.945(13)−3.065(8) Å. The distance between the metal center and the bridgehead carbon atom C(9) of the central ring is much larger than the Y−Cp_{Flu} bond lengths of 2.56(2)−2.74(2) Å observed in (η^5:η^5-Cp−$SiMe_2$−Flu)Y($N(SiMe_3)_2$) and (η^5:η^3-Cp−$SiMe_2$−Flu)$YCl_2Li(OEt_2)_2$.[12] Nonetheless, as developed in the next section, effective bonding between Y and C(9) is clearly established from the computed Mulliken overlap populations obtained by single-point calculations on the three polymorphs, as well as on the optimized geometry of **2**. The other fluorenyl moiety in the three polymorphs of **2** differs from the first one in that the yttrium−carbon bond distances to C(34), C(40), and C(39) are 2.671(8)−2.722(6), 3.101(7)−3.177(8), and 3.540(8)−3.633(12) Å, respectively. These metric data, that is, the difference of more than 0.8 Å between the shortest and the longest bond distances, and of 0.4−0.5 Å between the shortest and medium bond distances, suggest that the second fluorenyl moiety is coordinated via a new bonding mode that involves merely one carbon atom of the phenyl ring (**E**, Chart 1). As developed hereafter, this η^1-bonding mode is also corroborated by our theoretical investigation.

The solid-state molecular structure of **3** features a closely associated ion pair (Figure 2). The counterion is presented by a lithium atom coordinated in a pseudo-trigonal fashion by two diethyl ether molecules and the five-membered ring of one fluorenyl moiety (Li(1)−C(17−21) = 2.393(13)−2.446(13) Å; torsion angle O−Li−O−Cp(centroid) = 160.6°). The overall structure of the anion resembles that of **2**, with the lanthanum atom coordinated in a distorted-tetrahedral geometry by a pair of [Flu−CMe_2−Cp] ligand units. At variance with **2**, in which only one fluorenyl moiety is coordinated in an exocyclic η^3 fashion while the other one is coordinated in a $\eta^1(\eta^2)$ fashion**,** both fluorenyl units of **3** are coordinated in this η^3-bonding mode, which involves the bridgehead carbon atom of the central five-membered ring (C(9) and C(39)) and the two adjacent atoms of one six-membered ring (C(10), C(4), and C(40), C(34)). This η^3 coordination of the two fluorenyl ligands is quite symmetric and approaches the ideal case (**D**), as shown

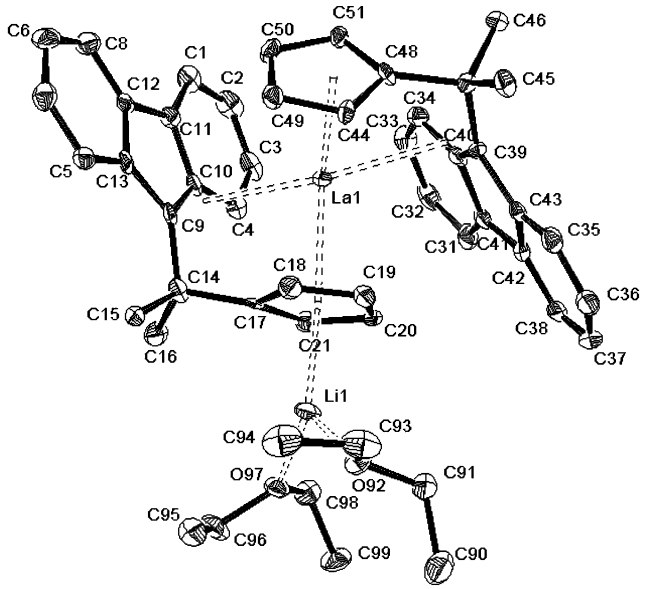

Figure 2. ORTEP drawing of [(η^3:η^5-Flu−CMe_2−Cp)$_2$La]$^-$-[$Li(OEt_2)_2$]$^+$ (**3**). All hydrogen atoms are removed for clarity; ellipsoids correspond to 50% probability.

by the small difference between the bond distances of La with the two terminus carbon atoms (Δ(La(1)−C(9)/La(1)−C(4)) = 0.028(7) Å; Δ(La(1)−C(34)/La(1)−C(39)) = 0.112(6) Å), a deviation likely attributable to the chelating constraints imposed by the isopropylidene bridge or crystal packing. The La−C(Flu) bond distances range from 2.881(7) to 3.077(6) Å and are longer than those involving the η^3-bonded fluorenyl moiety (C(4)−C(10)−C(9)) in the yttrium analogue **2** and in [(η^5:η^3-Cp−CMe_2−Flu)Zr(μ-H)(Cl)]$_2$,[15] as expected from a major influence of effective ionic radii of the metal centers.[9] These distances are also logically slightly longer than those observed in species with higher hapticity, e.g. [(η^5:η^5-Cp−CPh_2−Flu)La(BH_4)$_2$][Li($THF)_4$] (2.788(3)−3.010(3) Å)[4a] and in the chelated ring of (η^5:η^5-Cp−CMe_2−Flu)La(η^5-Cp−CMe_2−FluH)(THF) (2.811(5)−2.997(6) Å).[5]

The data of Table 2 show that the geometrical parameters for complexes **2** and **3** with the [Cp−CMe_2−Flu] ligand are rather uniform. The inner angle ϕ at the bridging carbon atom (C(14) and C(44); 108.7 ± 0.7° in **2**, 108.3 ± 0.1° in **3**) is somewhat larger than ϕ in related complexes, e.g. [(η^5:η^5-Cp−CPh_2−Flu)La(BH_4)$_2$]-[Li($THF)_4$] (104.1(2)°)[4a] and (η^5:η^5-Cp−CMe_2−Flu)La(η^5-$CpCMe_2$FluH)(THF) (104.7(4)°),[5] consistent with higher steric hindrance at the metal center due to the presence of two chelating ligands. The larger bite angles in the chelate ring Flu−Ln−Cp observed in **2** vs **3** are as expected from the ionic radii.[9]

The molecular structure of **4** comprises a fully dissociated ion pair in the solid state (Figure 3). The cation is composed by a lithium atom coordinated by four THF molecules,[4] and the anion consists of an yttrium atom coordinated in a distorted-tetrahedral geometry by two equivalent [Ind−CMe_2−Ind] ligand units. In contrast to fluorenyl-containing complexes **2** and **3**, only the cyclopentadienyl rings of the indenyl moieties coordinate to yttrium in **4**. The Y−C(Cp) bond distances are in the range of 2.524(5)−3.130(5) Å with the two bridging carbon atoms (C(1), C(6); C(14), C(19)) being farther away from the metal center. The difference of ca. 0.2−0.3 Å between these longest bond distances involving

(15) Bochmann, M.; Lancaster, S. J.; Hursthouse, M. B.; Mazid, M. *Organometallics* **1993**, *12*, 4718.

(16) A similar exocyclic η^3 coordination of fluorenyl ligands has been observed in the solid-state structures of alkaline-earth-metal complexes (η^3:η^3-$FluSiMe_2Flu)_2M(THF)_n$ (M = Ca, n = 3; M = Ba, n = 4): Harder, S.; Lutz, M.; Straub, W. G. *Organometallics* **1997**, *16*, 107.

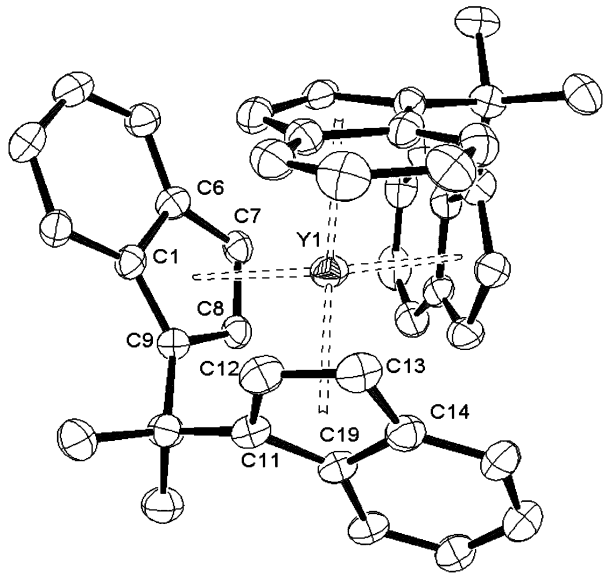

Figure 3. ORTEP drawing of the anion of $[(\eta^3{:}\eta^3\text{-Ind}-CMe_2-\text{Ind})_2Y]^-[Li(THF)_4]^+(THF)$ (**4**·THF). All hydrogen atoms are removed for clarity; ellipsoids correspond to 50% probability. Selected bond distances (Å) and angles (deg): C(9)−Y(1), 2.766(5); C(8)−Y(1), 2.565(5); C(7)−Y(1), 2.784(5); C(6)−Y(1), 3.130(5); C(1)−Y(1), 3.106(5); Cp(1)−Y(1), 2.608(5); C(11)−Y(1), 2.742(6); C(12)−Y(1), 2.611(6); C(13)−Y(1), 2.738(6); C(14)−Y(1), 2.948(5); C(19)−Y(1), 2.949(5); Cp(11)−Y(1), 2.524(5); C(9)−C(10)−C(11), 103.1(4); Cp(1)−Y(1)−Cp(2), 92.9 (Cp(1) is the centroid of C(1)−C(6)−C(7)−C(8)−C(9); Cp(2) is the centroid of C(11)−C(12)−C(13)−C(14)−C(19)).

the latter bridging carbon atoms and the other ones indicates that each of the four cyclopentadienyl rings tends to approach reduced hapticity (η^3 bonding mode).[17] Assuming that the metal atom bonded in an unambiguous η^3 mode to four fluorenyl units would correspond to a 16-electron count on a complex of the ML_8 general type. This is unlikely for such a nonplanar complex. Rather, we suggest taking into account the partial (highly unsymmetrical) η^5 hapticity of the C_5 rings and to consider the anion of **4** as an 18-electron species.

DFT Calculations on the Anion of 2, $[(Flu-CMe_2-Cp)_2Y]^-$, and General MO Considerations. To get a better understanding of the unusual bonding modes observed in these bis(chelated) anionic lanthanidocenes, density functional theory (DFT) calculations were carried out on the anion of **2**. Single-point calculations have been performed on the three experimental molecular structures of the complex $[(Flu-CMe_2-Cp)_2Y]^-$, which correspond to the three polymorphic varieties of **2**. As expected, the three computed structures exhibit similar electronic properties, as exemplified by their major computed data given in Table 3. Clearly, the Y−C Mulliken overlap populations confirm

Table 3. Major Computed DFT Data for the $[(Flu-CMe_2-Cp)_2Y]^-$ Anion, Assuming the Experimental Structures of the Polymorphs of 2 (Single-Point Calculations), and for the Fully Optimized Geometry

HOMO−LUMO gap (eV)			
monoclinic **2**	triclinic **2**	orthorhombic **2**	optimized geom
1.56	1.37	1.47	1.63

	10^4(MOP)[a]				
	monoclinic **2**	triclinic **2**	orthorhombic **2**	optimized geom	dist (Å)
Ln(1)−C(4)	70	57	57	70	2.835
Ln(1)−C(10)	96	96	89	74	2.904
Ln(1)−C(9)	62	66	71	51	3.138
Ln(1)−C(34)	109	120	107	108	2.823
Ln(1)−C(40)	77	70	73	50	3.188
Ln(1)−C(39)	27	6	22	15	3.604
Ln(1)−C(17−21)[b]	51	58	57	47	2.685
Ln(1)−C(47−51)[b]	55	52	53	45	2.696

Mulliken net charges				
	monoclinic **2**	triclinic **2**	orthorhombic **2**	optimized geom
Ln(1)	1.03	1.03	1.02	1.15
C(4)	0.13	0.16	0.14	0.02
C(10)	0.02	0.00	0.00	0.02
C(9)	−0.02	−0.05	−0.03	0.02
C(34)	0.07	0.06	0.06	−0.05
C(40)	0.07	0.08	0.07	0.08

[a] MOP = Mulliken overlap population. [b] Average value.

the $\eta^1(\eta^2)$ bonding mode with C(34) and C(40), C(34) being much more strongly bound to Y than C(40). A very weak bonding interaction between Y and C(39) can also be traced in the monoclinic and orthorhombic varieties, despite the large values of the corresponding interatomic separations (3.5−3.6 Å). However, one should note that the Y−C(39) overlap population is small compared to those corresponding to the C_5 rings, while the Y−C(40) overlap population, which amounts to about half of that obtained for Y−C(34), is significantly larger than the Y−C(C_5) populations. Therefore, one can describe the bonding mode of the corresponding fluorenyl moiety as being a new $\eta^1(\eta^2)$ mode that involves primarily one carbon atom of the phenyl ring (**E**, Chart 1). The asymmetric η^3-allyl bonding mode of Y with C(4), C(10), and C(9) is also confirmed by the calculations. In particular, the effective bonding between Y and C(9) is clearly established from the significant values of the corresponding overlap populations (0.06−0.07). The bonding of Y with C(10) is significantly stronger than that with C(4) and C(9), even in the orthorhombic variety, in which Y−C(10) is longer than Y−C(4).

Full geometry optimizations of $[(Flu-CMe_2-Cp)_2Y]^-$ under C_1 symmetry have also been carried out. Three starting geometries have been considered, which correspond to the three experimental structures found in the three polymorphic varieties of **2**. The three resulting optimized geometries were found to lie within an insignificant energy range of 0.023 eV, with some small metrical differences. For example, the Y−C bond distances lie in the range (in percent) of 3, 2, 5, 1, 4, and 5 for C(4), C(10), C(9), C(34), C(40), and C(39), respectively. Thus, the smallest variations occur on the carbon atoms that are the most strongly bonded to the metal. These results are indicative of a soft potential energy surface around the minimum. This is in agreement with

(17) The Y−C(Cp) bond distances of 2.524(5)−2.784(5) Å in **4**, considering an η^5 coordination, compare well with values found in other yttrocene compounds. (a) $Cp^*_2Y[N(SiMe_3)_2]$ (2.632(7)−2.737(7) Å): den Haan, K. H.; de Boer, J. L.; Teuben, J. H.; Spek, A. L.; Kojic-Prodic, B.; Hays, G. R.; Huis, R. *Organometallics* **1986**, *5*, 1726. (b) Cp_3Y·THF (2.65(1)−2.766(7) Å): Rodgers, R. D.; Atwood, J. L.; Emad, A.; Sikora, P. J.; Rausch, M. D. *J. Organomet. Chem.* **1981**, *216*, 383. (c) $[(C_5H_4Me)_2Y(\mu\text{-H})\cdot THF]_2$ (2.67(1)−2.71(1) Å): Evans, W. J.; Meadows, J. H.; Wayda, A. L.; Hunter, W. E.; Atwood, J. L. *J. Am. Chem. Soc.* **1983**, *104*, 2008−2014. (d) $Cp^*_2Y(\mu\text{-Cl})YClCp^*_2$ (2.56(2)−2.69(2) Å): Evans, W. J.; Peterson, T. T.; Rausch, M. D.; Hunter, W. E.; Zhang, H.; Atwood, J. L. *Organometallics* **1985**, *4*, 554.

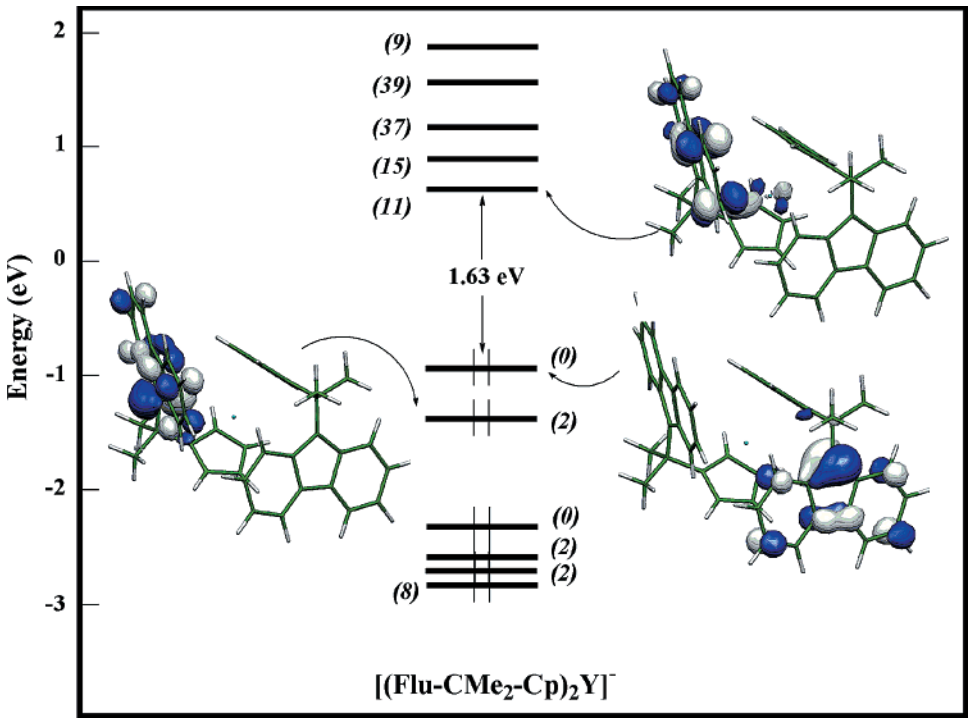

Figure 4. MO energy diagram and plots of the frontier orbitals of the anion of **2** (optimized geometry). Values in parentheses indicate the metal participation (in percent).

the existence of three different crystal structures of **2** and with its fluxional behavior in solution (see below).

Only the results corresponding to the lowest computed energy are reported in Table 3. The optimized geometry resembles the experimental structures, with similar structural and electronic features. One can only notice that the $\eta^1(\eta^2)$ and the η^3-allyl bonding modes are found somewhat more asymmetric in the optimized geometry, as compared to the crystal features. The geometry optimization confirms that the coordination of C(34) is planar (sum of the bond angles around C(34) 359.4°), indicating that the coordinated fluorenyl moiety to which it belongs remains fully conjugated. Therefore, C(34) (and to a lesser extent C(40)) is purely π-bonded to the metal. In this sense, bonding mode **E** can be seen as a limiting form of bonding mode **D**, with the π electron pair localized on the terminal phenyl carbon atom. As the two Cp rings are η^5-coordinated, the anion $[(\eta^3{:}\eta^5\text{-Flu}-\text{CMe}_2-\text{Cp})(\eta^1{:}\eta^5\text{-Flu}-\text{CMe}_2-\text{Cp})\text{Y}]^-$ is thus best formally described as an 18-electron complex of the general d^0 ML_9 type. This is corroborated by the large computed HOMO−LUMO gap (1.63 eV) and the absence of any vacant low-lying metallic MO, which would have indicated electron deficiency, as can be seen in the MO level diagram shown in Figure 4. It is consistent with this description that there is neither experimental nor computational evidence for an agostic Y−H interaction (shortest computed Y···H distance 2.80 Å). The two highest occupied MO's are derived from the HOMO's of the two fluorenyl moieties, whereas the two lowest vacant MO's are derived from the LUMO's of the fluorenyl moieties. Being significantly antibonding, the 4d-type levels are lying above these ligand-based MO's. Although the metal formal oxidation state is +III, the computed Mulliken net charge is +1.17, corresponding to the $d^{1.42}s^{0.12}p^{0.31}$ valence electron configuration. This is indicative of significant metal−ligand covalent interaction. Consistently, a decomposition of the bonding energy[18] between Y^{3+} and the $[(\text{Flu}-\text{CMe}_2-\text{Cp})_2]^{4-}$ fragment led to a significant orbital interaction component of −24.37 eV for a total bonding energy of −59.68 eV (the Pauli repulsion and electrostatic interaction components are 5.23 and −40.55 eV, respectively).

At this stage of the discussion, it is worth returning to the major difference between the solid-state structures of **2** and **3**. In $[(\text{Flu}-\text{CMe}_2-\text{Cp})_2\text{Y}]^-$, Y is coordinated in an η^3 fashion with one fluorenyl ligand and in an $\eta^2(\eta^1)$ fashion with the other one. In $[(\text{Flu}-\text{CMe}_2-\text{Cp})_2\text{La}]^-$, both fluorenyl units are coordinated in the η^3 bonding mode. Thus, following the way we described the former as an 18-electron complex, one might be tempted to erroneously describe the latter as a 20-electron species. Actually, one should remember that in the crystal structure of **3**, one of the Cp ligands is bonded in a η^5 fashion not only to La (as the other one) but also to the Li atom (Figure 2). As a consequence, two π electrons of this Cp ligand are not donated to La but to Li, so that $[(\text{Flu}-\text{CMe}_2-\text{Cp})_2\text{La}]^-$ should be described as a 18-electron complex.

Solution Structure of Ionic Complexes $[(\text{Flu}-\text{CMe}_2-\text{Cp})_2\text{Y}]^-[\text{Li}(\text{Et}_2\text{O})(\text{THF})_3]^+$ (2) and $[(\text{Flu}-\text{CMe}_2-\text{Cp})_2\text{La}]^-[\text{Li}(\text{Et}_2\text{O})_2]^+$ (3). The ^{1}H NMR spectrum of **2** in THF-d_8 at room temperature displays broadened resonances. At −30 °C, four sharp resonances typical for the fluorenyl protons (two virtual doublets from the ortho protons of the six-membered rings and two virtual triplets from the corresponding meta protons), two relatively broad signals from the AA′XX′ spin system of the monosubstituted Cp system, and one sharp six-proton singlet for the CMe_2 bridge are ob-

(18) (a) Ziegler, T.; Rauk, A. *Theor. Chim. Acta* **1977**, *46*, 1. (b) Ziegler, T.; Rauk, A. *Inorg. Chem.* **1979**, *18*, 1558. (c) Ziegler, T.; Rauk, A. *Inorg. Chem.* **1979**, *18*, 1755. (d) Bickelhaupt, F. M.; Baerends, E. J. *Rev. Comput. Chem.* **2000**, *15*, 1−86.

served. This pattern is consistent with a symmetric coordination of both of the [Flu−CMe_2−Cp] moieties to the metal center on the NMR time scale. It suggests rapid exchange of bonding modes **D** and **E** between the two fluorenyl moieties and/or rapid symmetrization of bonding within each fluorenyl moiety via slippage from one six-membered ring to the one opposite. The room-temperature ^{1}H NMR spectrum of lanthanum complex **3** in THF-d_8 reveals the same pattern of resonances as for **2**, diagnostic of a symmetric structure on the NMR time scale, with a six-proton methyl singlet, two non-resolved resonances from the Cp protons, and four well-dispersed fluorenyl protons. This is consistent with dissociation of the ion pair in **3** in solution and indicates that both yttrium and lanthanum [(Cp−CMe_2−Flu)$_2$-Ln]$^-$ anion fragments have comparable behaviors. In agreement with this symmetry in solution, the ^{13}C NMR spectra of **2** and **3** show each a single set of 12 resonances. The bridgehead carbon C(9)/C(39) appears at 103.5 ppm in **2** and at 95.9 ppm in **3**.[19] These values can be compared to the chemical shift of 95.4 ppm reported for the corresponding carbon in [(η^5:η^3-Cp−CMe_2−Flu)Zr(μ-H)(Cl)]$_2$[15] and suggests that reduced hapticity (η^3 modes **D**/**E**) is conserved for species **2** and **3** in solution.[19]

Conclusion

In conclusion, we have shown that yttrium and lanthanum, two quite differently sized group III metal centers, can effectively accommodate in their coordination sphere two bulky chelating [Cp−CMe_2−Flu] ligand units. The fluorenyl moieties in these anionic complexes adopt, in the solid state, dissymmetric bonding delocalized over the phenyl rings with a reduced hapticity. It would appear likely that these unusual bonding features originate from the combination of steric crowding at the metal center, the constraints within the ligand imposed by the one-carbon bridge and the limited electron availability of Ln^{3+}. The identification of three polymorphic varieties of the yttrium complex and DFT computations show that such modes of coordination are indeed rather flexible.

Experimental Section

General Considerations. All manipulations were performed under a purified argon atmosphere using standard Schlenk techniques or in a glovebox. Solvents were distilled from Na/benzophenone (THF, Et_2O) and Na/K alloy (toluene, pentane) under nitrogen, degassed thoroughly, and stored under nitrogen prior to use. Deuterated solvents (benzene-d_6, toluene-d_8, THF-d_8; >99.5% D, Eurisotop) were vacuum-transferred from Na/K alloy into storage tubes. $YCl_3(THF)_{3.5}$ and $LaCl_3(THF)_{1.5}$ were obtained after repeated extraction of YCl_3 and $LaCl_3$ (Strem) from THF or just prior to use by reflux of the anhydrous lanthanide chloride in THF for 2 h and subsequent evaporation. The ligands CpH−CMe_2−FluH and IndH−CMe_2−IndH were generously provided by TotalFinaElf. NMR spectra were recorded on Bruker AC-200, AC-300, and AM-500 spectrometers in Teflon-valved NMR tubes at 23 °C, unless otherwise indicated. ^{1}H and ^{13}C chemical shifts are reported vs $SiMe_4$ and were determined by reference to the residual solvent peaks. Assignment of signals was made from ^{1}H−^{1}H COSY, ^{1}H−^{13}C HMQC, and HMBC NMR experiments. Coupling constants are given in hertz. Elemental analyses were performed by the Microanalytical Laboratory at the Institute of Chemistry of Rennes and are the average of two independent determinations. Micro X-ray fluorescence analysis was carried out using an Eagle-II (Röntgenanalytik Messtechnik GmbH, Taunusstein, Germany) energy dispersive spectrometer equipped with a Mo X-ray tube. Standardless quantitative analysis employed the Vision XRF version 3.35 software. A batch of grains of polycrystalline material was sandwiched between thin polyacetate films. Individual grains were selected by optical inspection and fluorescence data from an area not exceeding 300 μm in diameter recorded. For qualitative and quantitative analysis only elements between Na and U can be measured and only Cl and Y were detected.

Salt Metathesis between [Flu−CMe_2−Cp]Li_2 and $YCl_3(THF)_{3.5}$ (1:1): Synthesis of "[(Cp−CMe_2−Flu)YCl_2]$^-$[Li(ether)$_4$]$^+$" (1; ether = Et_2O, THF). To a solution of $C_{13}H_8H$−CMe_2−C_5H_4H (1.00 g, 3.67 mmol) in Et_2O (50 mL) at −10 °C was added under vigorous stirring 2 equiv of *n*-BuLi (4.6 mL of a 1.6 M solution in hexane, 7.34 mmol). The reaction mixture was warmed to room temperature. The solution turned dark yellow, and after 3 h a yellow crystalline powder precipitated. To this suspension of the dilithium salt in ether cooled to −20 °C was added a suspension of $YCl_3(THF)_{3.5}$ (prepared from 0.72 g, 3.68 mmol of YCl_3) in Et_2O (50 mL). Upon vigorous stirring and warming to ambient temperature, the reaction mixture turned deep red. The solution was decanted from the precipitate, filtered, and evaporated in vacuo to give a deep red powder (1.75 g, 65% yield). ^{1}H NMR (200 MHz, THF-d_8, 70 °C): δ 8.16 (d, 2H, J_{HH} = 7.3, Flu), 7.48 (m, 2H, Flu), 7.25 (m, 2H, Flu), 6.71 (t, 2H, J_{HH} = 7.3, Flu), 5.25 (s, 2H, Cp), 4.09 (br s, 2H, Cp), 3.39 (q, 4H, α-CH_2, Et_2O), 1.76 (s, 6H, CCH_3, overlap with solvent resonances), 1.10 (t, 4H, α-CH_2, Et_2O). Anal. Calcd for $C_{37}H_{52}Cl_2LiO_4Y$ "([(Cp−CMe_2−Flu)YCl_2][Li(Et_2O)$(THF)_3$])" (727.57): C, 61.08; H, 7.20. Found: C, 59.92; H, 6.92. Recrystallization of this crude product from an Et_2O/THF (10:1) solution at −30 °C afforded dark red crystals of [(Flu−CMe_2−Cp)$_2$Y]$^-$[Li(Et_2O)$(THF)_3$]$^+$ (**2**; 0.80 g, 47% yield vs ligand) (vide infra).

Synthesis of [(Flu−CMe_2−Cp)$_2$Y]$^-$[Li(Et_2O)$(THF)_3$]$^+$ (2). To a solution of $C_{13}H_8H$−CMe_2−C_5H_4H (0.200 g, 0.734 mmol) in Et_2O (30 mL) at −10 °C was added with vigorous stirring 2 equiv of *n*-BuLi (0.92 mL of a 1.6 M solution in hexane, 1.47 mmol). The reaction mixture was warmed to room temperature. The solution turned dark yellow, and after 3 h a yellow crystalline powder precipitated. To this suspension of the dilithium salt in ether cooled to −20 °C was added a suspension of $YCl_3(THF)_{3.5}$ (prepared from 0.072 g, 0.368 mmol of YCl_3) in Et_2O (20 mL). Upon vigorous stirring and warming to room temperature the reaction mixture turned deep red. The red solution was decanted and separated from the precipitate, concentrated in vacuo, and cooled to −20 °C to yield highly air-sensitive deep red crystals of **2** (0.237 g, 70%). ^{1}H NMR (300 MHz, THF-d_8, −30 °C): δ 7.86 (d, 4H, J_{HH} = 7.3, Flu), 7.20 (d, 4H, J_{HH} = 7.3, Flu), 6.69 (t, 4H, J_{HH} = 7.3, Flu), 6.31 (t, 4H, J_{HH} = 7.3, Flu), 5.66 (br s, 4H, Cp), 4.50 (br s, 4H, Cp), 3.57 (br s, 12H, α-CH_2, THF), 3.33 (q, 4H, α-CH_2, Et_2O), 1.84 (s, 12H, C(CH_3)$_2$), 1.73 (br s, 12H, β-CH_2, THF), 1.07 (t, 4H, α-CH_2, Et_2O). ^{1}H NMR (200 MHz, THF-d_8, 70 °C): δ 8.18 (d, 4H, J_{HH} = 7.3, Flu), 7.51 (d, 4H, J_{HH} = 7.3, Flu), 7.30 (t, 4H, J_{HH} = 7.3, Flu), 6.74 (t, 4H, J_{HH} = 7.3, Flu), 5.21 (br s, 4H, Cp), 4.06 (br s, 4H, Cp), 3.39 (q, 4H, α-CH_2, Et_2O), 1.73 (br s, 6H, CH_3, overlap with solvent resonances), 1.10 (t, 4H, α-CH_2, Et_2O). ^{1}H{^{13}C} NMR (75 MHz, THF-d_8, −30 °C): 140.5 (Cp), 132.9 (Flu-10,13 or Flu-11,12), 124.5 (Flu-11,12 or Flu-10,13), 120.4 (Flu-2,7 or Flu-3,6), 119.1 (Flu-1,8 or Flu-4,5), 113.6 (Flu-4,5 or Flu-1,8), 110.5 (CH Cp), 108.1 (CH Cp), 108.0 (Flu-3,6 or Flu-2,7), 103.5 (Flu-9), 66.3 (CH_3CH_2O, Et_2O), 39.3 (CH_3C), 32.2 (CH_3C), 15.7 (CH_3CH_2O, Et_2O). Anal. Calcd for $C_{58}H_{70}LiO_4Y$ (927.04): C, 75.14; H, 7.61; Found: C, 75.43; H, 7.92.

(19) Drago, D.; Pregosin, P. S.; Razavi, A. *Organometallics* **2000**, *19*, 1802.

Salt Metathesis between [Flu−CMe_2−Cp]Li_2 and $LaCl_3(THF)_{1.5}$ (1:1): Synthesis of [(Cp−CMe_2−Flu)$LaCl_2$]$^-$[Li$(Et_2O)_2$]$^+$ (3). To a solution of $C_{13}H_8H-CMe_2-C_5H_4H$ (0.310 g, 1.135 mmol) in Et_2O (20 mL) at −10 °C was added under vigorous stirring 2 equiv of *n*-BuLi (1.42 mL of a 1.6 M solution in hexane, 2.27 mmol). The reaction mixture was warmed to room temperature. The solution turned dark yellow, and after 3−4 h a yellow crystalline powder precipitated. To this suspension of the dilithium salt in ether cooled to −20 °C was added a suspension of $LaCl_3(THF)_{1.5}$ (prepared from 0.279 g, 1.135 mmol of $LaCl_3$) in Et_2O (20 mL). Upon vigorous stirring and warming to room temperature the reaction mixture turned pink. The solution was decanted from the precipitate, filtered, and kept at −35 °C to give highly air-sensitive pink crystals of **3** (0.20 g, 42% yield vs ligand). ^{1}H NMR (200 MHz, THF-d_8, 60 °C): δ 8.04 (d, 4H, J_{HH} = 7.5, Flu), 7.42 (d, 4H, J_{HH} = 7.5, Flu), 6.91 (t, 4H, J_{HH} = 7.5, Flu), 6.65 (t, 4H, J_{HH} = 7.5, Flu), 5.36 (br s, 4H, Cp), 4.18 (br s, 4H, Cp), 3.36 (q, 8H, Et_2O), 1.75 (s, 12H, CH_3, overlapped with THF), 1.07 (q, 12H, Et_2O). ^{1}H NMR (300 MHz, THF-d_8, 25 °C): δ 8.04 (d, 4H, J_{HH} = 7.3, Flu), 7.42 (br s, 4H, Flu), 6.91 (t, 4H, J_{HH} = 7.3, Flu), 6.66 (t, 4H, J_{HH} = 7.3, Flu), 5.38 (br s, 4H, Cp), 4.6−3.7 (br s, 4H, Cp), 3.34 (q, 8H, Et_2O), 1.68 (s, 12H, CH_3, overlap with solvent resonances), 1.07 (q, 12H, Et_2O). ^{13}C{^{1}H} NMR (300 MHz, THF-d_8, 25 °C): δ 134.2, 126.0, 124.7 (CH Flu), 120.5 (CH Flu), 113.2 (CH Flu), 112.0 (CH Flu), 108.0 (Cp), 95.9 (Flu-9), 66.2 (CH_2, Et_2O), 39.0 (CCH_3), 26.3 (CCH_3), 15.6 (CH_3, Et_2O) (the signal from the ipso carbon of Cp moieties was not observed). Anal. Calcd for $C_{50}H_{56}O_2$LaLi (834.84): C, 71.93; H, 6.76. Found: C, 71.58; H, 7.06.

Synthesis of [(Ind−CMe_2−Ind)$_2$Y]$^-$[Li$(THF)_4$]$^+$(THF) (4). To a solution of $C_9H_6H-CMe_2-C_9H_6H$ (0.408 g, 1.50 mmol) in Et_2O (40 mL) at −10 °C was added under vigorous stirring 2 equiv of *n*-BuLi (1.87 mL of a 1.6 M solution in hexane, 3.00 mmol). The reaction mixture was warmed to room temperature. To the resulting pale yellow solution of the dilithium salt in ether cooled to −20 °C was added a suspension of $YCl_3(THF)_{3.5}$ (0.335 g, 0.75 mmol) in Et_2O (20 mL). Upon vigorous stirring and warming to ambient temperature the reaction mixture turned dark yellow with concomitant precipitation of LiCl. The dark yellow solution was decanted from precipitate, filtered, concentrated in vacuo, and cooled to −35 °C to give yellow crystals of **4** (0.61 g, 88% yield). ^{1}H NMR (500 MHz, THF-d_8, 25 °C): δ 7.87 (d, 4H, J_{HH} = 8.5, Ind), 7.08 (d, 4H, J_{HH} = 8.5, Ind), 6.69 (t, 4H, J_{HH} = 8.5, Ind), 6.57 (t, 4H, J_{HH} = 8.5, Ind), 5.52 (d, 4H, J_{HH} = 8.5, Ind−Cp), 4.05 (d, 4H, J_{HH} = 8.5, Ind−Cp), 2.01 (s, 12H, CH_3). ^{13}C{^{1}H} NMR (125 MHz, THF-d_8, 25 °C): δ 130.5, 130.16, 124.43, 122.17, 121.78, 117.62, 117.22, 111.08, 97.03, 40.12 (CCH_3), 31.49 (CCH_3). Anal. Calcd for $C_{58}H_{68}LiO_4Y$ (**4**; 925.00): C, 75.31; H, 7.41. Found: C, 75.08; H, 7.62. X-ray-quality crystals were grown from an Et_2O/THF solution at −30 °C.

Crystal Structure Determination of Complexes 2−4. Suitable single crystals of all investigated compounds were mounted onto glass fibers using the "oil-drop" method. All diffraction data were collected at 100−120 K using a NONIUS Kappa CCD diffractometer with graphite-monochromatized Mo Kα radiation (λ = 0.710 73 Å). A combination of ω and φ scans was carried out to obtain at least a unique data set. Crystal structures were solved by means of the Patterson method, and the remaining atoms were located from difference Fourier synthesis, followed by full-matrix least-squares refinement based on F^2 (programs Shelxs-97 and Shelxl-97).[20] Many hydrogen atoms could be found from the Fourier difference; this includes in particular the hydrogen atoms on the phenyl carbon atoms C(34) and C(4) of the fluorenyl ligands in the three polymorphs of **2** and in **3**. Conversely, no hydrogen atoms could be localized around the bridgehead carbon atoms C(9) and C(39) of the central ring in these structures. Carbon-bound hydrogen atoms were placed at calculated positions and forced to ride on the attached carbon atom. The hydrogen atom contributions were calculated but not refined. All non-hydrogen atoms were refined with anisotropic displacement parameters. The locations of the largest peaks in the final difference Fourier map calculation as well as the magnitude of the residual electron densities were of no chemical significance. The cell of triclinic **2** was found to contain one diethyl ether molecule of crystallization and that of **4** one THF molecule of crystallization. Crystal data and details of data collection and structure refinement are given in Table 1. Atomic coordinates, thermal parameters, and complete listings of bond lengths and angles are available as Supporting Information.

Computational Details. DFT calculations were carried out with the Amsterdam Density Functional (ADF) program (release 2.3)[21] developed by Baerends and co-workers.[22] Electron correlation was treated within the local density approximation (LDA) in the Vosko−Wilk−Nusair parametrization.[23] The nonlocal corrections of Becke[24] and Perdew[25] were added to the exchange and correlation energies, respectively. The numerical integration procedure used in the calculations was developed by te Velde et al.[21] The standard ADF STO basis set IV was used; i.e., a triple-ζ Slater-type orbital (STO) basis for Y 4d and 5s and a single-ζ function for Y 5p. A triple-ζ STO basis set was also employed for H 1s and for C 2s and 2p, extended with a 2p and 3d single-ζ polarization function for H and C, respectively. The frozen-core approximation was considered. The decomposition of the bonding energy between Y^{3+} and its ligand sphere was done according to the method of Ziegler and Rauk.[18]

Acknowledgment. This work was financially supported by TotalFinaElf (grant to E.K.). We are most grateful to Vincenzo Bellia for technical support. Computing facilities were provided by the Centre de Ressources Informatiques (CRI) of Rennes and the Institut de Développement et de Ressources en Informatique Scientifique du Centre National de la Recherche Scientifique (IDRIS-CNRS).

Supporting Information Available: Details of structure determinations of complexes **2** (three polymorphic varieties), **3**, and **4**, including final coordinates, thermal parameters, bond distances, and bond angles. This material is available free of charge via the Internet at http://pubs.acs.org. Crystallographic data for the three polymorphic varieties of **2** have also been deposited with the Cambridge Crystallographic Data Centre under the reference numbers CCDC-201334, -201335, and -201336. These data can be obtained free of charge on application to the CCDC, 12 Union Road, Cambridge CB2 1EZ, U.K. (fax, (+44) 1223 336-033; e-mail, deposit@ccdc.cam.ac.uk).

OM030181O

(20) (a) Sheldrick, G. M. SHELXS-97, Program for the Determination of Crystal Structures; University of Göttingen, Göttingen, Germany, 1997. (b) Sheldrick, G. M. SHELXL-97, Program for the Refinement of Crystal Structures; University of Göttingen, Göttingen, Germany, 1997.

(21) (a) te Velde, G.; Bickelhaupt, F. M.; van Gisbergen, S. J. A.; Fonseca Guerra, C.; Baerends, E. J.; Snijders, J. G.; Ziegler, T. *J. Comput. Chem.* **2001**, *22*, 931. (b) Fonseca Guerra, C.; Snijders, J. G.. te Velde, G.; Baerends, E. J.; *Theor. Chim. Acta* **1998**, *98*, 391. (c) Amsterdam Density Functional Program (ADF 2000.03); SCM, Division of Theoretical Chemistry, Vrije Universiteit, De Boelelaan 1083, 1081 HV Amsterdam, The Netherlands; http://www.scm.com.

(22) (a) Baerends, E. J.; Ellis, D. E.; Ros, P. *Chem. Phys.* **1973**, *2*, 41. (b) Baerends, E. J.; Ros, P. *Int. J. Quantum Chem.* **1978**, *S12*, 169. (c) Boerringter, P. M.; te Velde, G.; Baerends, E. J. *Int. J. Quantum Chem.* **1988**, *33*, 87. (d) te Velde, G.; Baerends, E. J. *Int. J. Quantum Chem.* **1992**, *99*, 84.

(23) Vosko, S. D.; Wilk, L.; Nusair, M. *Can. J. Chem.* **1990**, *58*, 1200.

(24) Becke, A. D. *Phys. Rev.* **1988**, *A38*, 3098.

(25) Perdew, J. P. *Phys. Rev.* **1986**, *B33*, 8822; **1986**, *B34*, 7406 (erratum).